

SPECIAL ISSUE ARTICLE **OPEN ACCESS**

Crosslinking Behavior of Ethylene-Vinyl Acetate Copolymer Encapsulants in Dependence of the Additive Composition

Michael Wendt¹  | Patrick Wessel^{1,2} | Ralph Gottschalg^{1,2}  | Anton Mordvinkin¹  | Robert Heidrich^{1,2} ¹Fraunhofer CSP, Halle (Saale), Germany | ²Department of Electrical Engineering, Mechanical Engineering and Industrial Engineering, Anhalt University of Applied Sciences, Koethen (Anhalt), Germany**Correspondence:** Robert Heidrich (robert.heidrich@csp.fraunhofer.de)**Received:** 28 June 2024 | **Revised:** 30 August 2024 | **Accepted:** 3 September 2024**Funding:** The authors received no specific funding for this work.**Keywords:** additives | crosslinking | DSC | encapsulant | EVA | gel content

ABSTRACT

The three-dimensional crosslinking of encapsulants in photovoltaic (PV) modules significantly defines their thermomechanical properties and is usually initiated using peroxides and crosslinking accelerators. However, it has been shown that excess peroxides lead to undesirable side reactions such as browning, which is directly linked to the PV module power losses. Therefore, the encapsulant formulation should be adjusted accordingly, on the one hand, keeping the peroxide concentration possibly low and, on the other hand, enabling a sufficiently high gel content (GC). This work investigates the basic interaction of the crosslinking peroxide Luperox TBEC and the crosslinking accelerator Perkalink 301 (TAIC) with differential scanning calorimetry (DSC), to address this issue. In addition, their reaction potential with the antioxidant butylhydroxytoluene (BHT) is investigated. It is shown that stabilizing additives can have an influence on the peroxide crosslinking process, which can affect the resulting crosslinking state and require optimization of the lamination conditions. The additive content of commercial PV encapsulants is quantified using pyrolysis gas-chromatography mass spectrometry (PY-GCMS). Subsequently, a number of films with different TBEC and TAIC contents are produced, and their GC is analyzed as a function of the additive concentrations and lamination conditions. A range of formulations leading to a GC > 75% was identified which can be used as a guidance for encapsulant manufacturers.

1 | Introduction

The requirements for encapsulants for photovoltaic (PV) modules were already defined by Czanderna and Pern in 1996 [1]. Essentially, they can be reduced to ensuring that the encapsulant protects the solar cell from environmental influences, guarantees mechanical stability, compensates for the various thermal expansion coefficients, enables optical coupling between the cell and the incident radiation, and insulates the solar cell electrically [1, 2]. In order to improve the properties of the encapsulants so that they meet the requirements mentioned, additives are added on the one hand and the polymers are crosslinked on the other (which usually also requires the use of additives)

[3–10]. Thus, the ethylene-vinyl acetate (EVA) copolymer and polyolefin elastomer (POE) encapsulants currently used in the PV industry are typically crosslinkable polymers to guarantee the required mechanical stability over a wide temperature range [3, 7, 8, 11–13]. Since many module failures are due to the failure of the polymer layers and the degradation behavior of the encapsulants is also determined by the degree of crosslinking, it is important to understand the crosslinking process in detail [12, 14–16].

This process is typically initiated by crosslinking peroxides such as Luperox TBEC and is supported by crosslinking accelerators such as Perkalink 301 (TAIC) [17–19]. The process is

This is an open access article under the terms of the [Creative Commons Attribution](https://creativecommons.org/licenses/by/4.0/) License, which permits use, distribution and reproduction in any medium, provided the original work is properly cited.

© 2024 The Author(s). Progress in Photovoltaics: Research and Applications published by John Wiley & Sons Ltd.

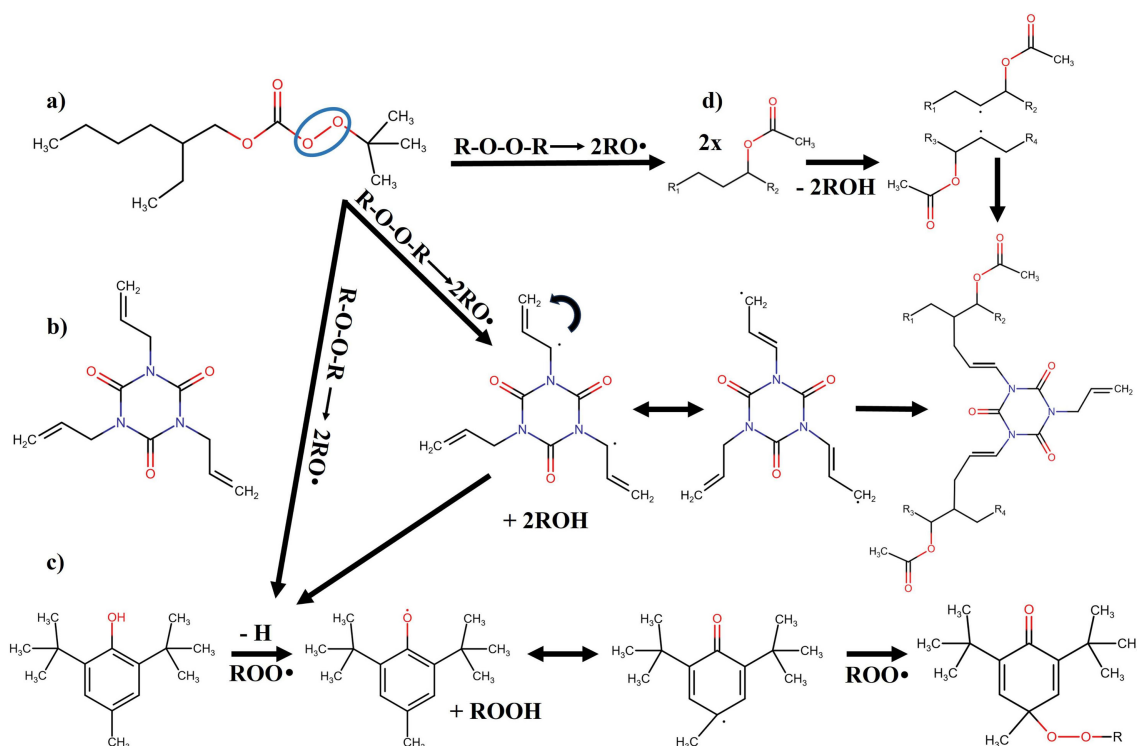


FIGURE 1 | Simplified functionality of the crosslinking peroxide Luperox TBEC (a), the crosslinking accelerator Perkalink 301 (TAIC) (b) and the antioxidant butylhydroxytoluene (BHT) (c) during the crosslinking process of EVA (d). The figure was adapted from [4] and is based on the work of [17–20].

shown schematically in Figure 1. The O–O bond of the crosslinking peroxide (a) is thermally cleaved and two radicals are formed [17, 18]. Through hydrogen abstraction, these radicals react either with the EVA chains or with the TAIC molecules (b) creating macro radicals [17–19, 21]. The generated radicals now recombine, and covalent bonds are formed between different polymer chains or between polymer chains and TAIC molecules, whereby the latter can be used as a bridge between EVA chains [17–19, 22, 23]. While Figure 1 shows the recombination of two polyethylene (PE) segments of EVA for the sake of simplicity. However, the covalent bonds could also form at the methyl group of the vinyl acetate (VA) segments [13, 24, 25].

However, the mode of action of peroxide crosslinking could lead to undesired interactions. Typically, radical scavengers are added to PV encapsulants to stabilize them and increase their service life [3, 5–10]. Especially, antioxidants such as butylhydroxytoluene (BHT) can already be present as process stabilizers in EVA granules [3]. Since the mode of action of the radical scavengers counteracts the radicals produced by the cleavage of the crosslinking peroxide, it is conceivable that the crosslinking process is influenced (see Figure 1c). However, to the best of our knowledge, there are no studies on the interactions of the additives used in this work during the crosslinking process of PV encapsulant.

Furthermore, most of the data on additive quantities used are based on the Flat-Plate Solar Array Project, which dates back almost 40 years [3, 5–8]. Crosslinking accelerators were not used in this work, and there are hardly any studies to date that deal with the influence of these additives in the PV sector. However, it is known that excess crosslinking peroxide can lead

to undesirable side effects such as browning of the encapsulant by reacting with UV absorber molecules which are creating chromophores [5, 12, 26, 27]. If the crosslinking accelerator has a positive effect on the expected gel content (GC) and fewer peroxides can therefore be used, the potential for undesirable side reactions is also decreasing.

The aim of this work is therefore to investigate the influence of the amount of crosslinking additives and their ratios on the crosslinking behavior of EVA. On the one hand, the reaction potential of the individual molecules TBEC, TAIC, and BHT is investigated in order to estimate their mutual influence. On the other hand, a previously developed method for quantifying additives is extended to crosslinking additives in order to determine the additive quantities currently used in commercial films [3]. Based on both preliminary experiments, a large number of EVA films has been produced in order to determine the necessary proportions of TBEC and TAIC for optimal crosslinking by minimizing the use of peroxides. Finally, the influence of the lamination temperature on the crosslinking behavior of selected film series is investigated, as the process conditions used can have a major influence on the long-term behavior of the films [12, 28].

2 | Methodology

2.1 | Additives and Polymer Matrix

The EVA film samples were produced in-house. Different mass fractions of the crosslinking agent (Luperox TBEC) and accelerator (Perkalink 301 - TAIC) were varied, while the fractions of the other additives (UV absorber, hindered amine light stabilizer - HALS,

TABLE 1 | Used EVA and additive amounts.

Name	Function	Amount (phr)	CAS
Evatane 18-25	EVA matrix	100	
Cyasorb UV 531	UV absorber	0.3	1843-05-6
Tinuvin 770	HALS	0.13	52829-07-9
Silane A174	Adhesion promoter	1.2	12530-85-0
Luperox TBEC	Crosslinking agent	0–1.45	34443-12-4
Perkalink 301	Crosslinking accel.	0–0.7	1025-15-6

Note: The mass fractions are based on the quantification within this work and the previous investigations of [3, 5–8].

and adhesion promoter) were kept constant and listed in Table 1 (see [supporting information](#) for a full list of all polymer films). The compositions are based on previous research whereby the quantities of crosslinking additives are based on those obtained by quantification using PY-GCMS of commercial foils (see Section 3.2) [3, 5–8]. EVATANE 28-25 with a vinyl-acetate content of 28wt% and a melting point of 71°C were used as EVA matrix. The properties are common for EVA encapsulants in the PV industry, and the low melting point is beneficial for the incorporation of the crosslinking additives in the kneader without its thermal activation [2, 29]. The EVA and additive compositions used to quantify the Luperox TBEC content in commercial films are based on ELVAX 150W, because this study was conducted in the past. However, ELVAX 150W has a comparable VA content and was used in the PV sector [6]. Consequently, the results should be transferable to commercial encapsulants. The properties of ELVAX 150W can be found in our previous work [3, 5].

2.2 | EVA Film Preparation

To achieve a good homogeneity of the additive distribution in the polymer matrix, the production of the raw polymer melt was carried out using a kneader. The various additives were precisely weighed and placed into small sample containers before the kneader was filled. The kneading was carried out in the Rheomix 600 kneader with the RheoDrive 7 as stirring unit. The kneader parameters were set to 70°C with 50 rpm for 5 min. A hydraulic press (Rucks KV 192.00) was used to produce the polymer films from the chunks. By using a stainless steel frame with 500- μ m thickness during the pressing process, films samples of a thickness of approximately 450 μ m were fabricated. Four sample films were produced in one press run. Pressing was carried out at 70°C and 200-bar pressure for 5 min. Figures of the preparation setup can be found in our previous publication [3].

2.3 | Lamination

A Meier ICOLAM 10/08 laminator was used for lamination. The lamination program consisted of three different stages and was based on the lamination of commercial films. In the later course of this work, the lamination peak temperature was varied to investigate its influence on the crosslinking behavior (see Section 3.4).

The laminator was preheated to 55°C. Afterwards, the EVA samples, protected on both sides by a PTFE release layer, were

inserted into the laminator. The evacuation and heating to 80°C took place within 6.5 min. Afterwards, the film samples were then further heated to 155°C while applying a pressure of 600 mbar. Temperature and pressure were maintained for a further 20 min. Finally, the samples were cooled to 55°C still applying the pressure of 600 mbar. To investigate the influence of temperature, additional laminations were carried out at 145°C and 165°C in Section 3.4.

2.4 | Characterization Methods

2.4.1 | Pyrolysis Gas-Chromatography Mass Spectrometry (PY-GCMS)

The quantification of the crosslinking additives was carried out using a PY-GCMS setup. The device and settings are explained in detail in our previous works [3–5]. The setup consists of an EGA/Py-3030D pyrolysis oven from Frontier Laboratories Ltd. with attached autosampler AS-1020E, a Trace 1300 gas chromatograph from Thermo Scientific with He carrier gas and an Ultra ALLOY Capillary Column (length 30 m, internal diameter 0.25 mm, film thickness 0.25 μ m) from Frontier Laboratories Ltd. An ISQ 7000 mass spectrometer from Thermo Scientific was coupled to the gas chromatograph, while the m/z range was set from 29 to 800.

2.4.2 | Differential Scanning Calorimetry (DSC)

The nonisothermal crosslinking experiments were carried out using a NETZSCH DSC 204 F1 PHOENIX. The heat flow versus temperature curves were measured in a temperature range of –40°C to 220°C under N₂ atmosphere (40 mL/min) at a heating rate of 10 K/min. The film samples were prepared using a 5-mm punch with sample masses of 6 to 8 mg weighed with a METTLER TOLEDO XS205DU (resolution of 0.01 mg and repeatability of 0.02 mg). The measurements were performed in 25- μ L aluminum crucibles. Every measurement was carried out in triple determination. All raw data were processed using OriginPro 2022b.

2.4.3 | GC Determination

The insoluble content (GC) was determined by using an in-house crosslinking test based on IEC standard 62788-1-6:2017 [30]. The samples are immersed in 12 mL of toluene in a test tube with rolled rim and snap-on lid. The extraction was carried

out in a drying cabinet at 80°C for 24 h, which extracts the uncrosslinked and soluble fraction of the EVA-polymer. Afterward, drying was carried out at 110°C for 12 h. The sample weight was measured before and after testing with the METTLER TOLEDO XS205DU (see above). The GC is calculated from the ratio of the residual mass m_{gel} and the initial mass m_0 according to [31]

$$GC = \frac{m_{gel}}{m_0}. \quad (1)$$

The film samples were prepared using a 7-mm punch with sample masses of approximately 15 mg. Every measurement was carried out in triple determination.

3 | Results and Discussion

3.1 | Interaction Potential of Pure Substances

Initially, the thermal decomposition of the pure substances and their mixtures were determined using nonisothermal measurements by DSC and visualized in the left image of Figure 2. The changes in heat flow and peak maximum temperatures were investigated. The thermograms enable a direct determination of the peak maximum temperature. The integration of the area of the exothermic reaction reflects the reaction enthalpy [32], which is normalized to the weight of TBEC as this is the only reactive substance. The conversion of the determined heat flow into the reaction enthalpy is based on the underlying constant heating rate. The exothermic reactions shown are typical for the decomposition of peroxidic systems [33]. In the case of the peroxide crosslinking agent TBEC, the thermal cleavage of the O–O bond takes place with the formation of two radicals [17, 18]. This process is associated with the release of energy [33]. The measured exothermic reaction heat of plain TBEC was approximately 685 J/g. The pure crosslinking accelerator TAIC shows no exothermic signal (see SI for DSC measurements). The combination of TAIC with the crosslinking agent TBEC (ratio 1:1) leads to an increase of the reaction enthalpy to approximately 1600 J/g. This

behavior can be explained by the transfer of the radical function from the TBEC to the trifunctional TAIC under formation of TAIC radicals [19]. The one-stage reaction of pure TBEC now becomes a two-stage reaction in the presence of TAIC. This behavior is typical for radical transfer reactions of TBEC and comparable to the transfer of the radical functionality to a solvent [33]. In addition to the formation of an additional shoulder, the temperature range from onset to final temperature also widens. This additive combination also showed a peak maximum temperature which was approximately 30 K lower than without crosslinking accelerators. Investigations at constant TBEC fraction and increasing TAIC fraction show a linear increase in the reaction enthalpy and are visualized in the right image of Figure 2. The x-axis shows the quotient of TAIC/TBEC. These studies confirm the radicalization of TAIC by thermally activated TBEC and the further transfer of radical functionalities among the TAIC molecules [19]. No limitation by either component could be detected in the concentration range investigated.

The addition of the antioxidant BHT to the crosslinking additives mixture significantly influences the measured total reaction heat and is displayed in Figure 3. Equivalent amounts of TAIC and TBEC (ratio 1:1) were used for these studies and supplemented with variable amounts of BHT. Depending on the concentration of BHT, the heat generated during thermal decomposition decreases from 1604 to 883 J/g. The onset temperature of the exothermic reaction is significantly shifted to higher temperatures from 82°C to 117°C. The comparison of the peak maximum temperatures shows, analogous to the onset temperatures, a clear shift towards higher temperatures. This can be explained by the fact that the previously described two-step reaction is attenuated by the presence of BHT and reverts to a one-step reaction like pure TBEC by eliminating the radical transfer reaction between TBEC and TAIC. BHT acts as a H-donor and radical scavenger [20]. The basic principle is the formation of hydroperoxides by transfer of a hydrogen from the phenolic molecule to the peroxy-radical [20] (see Figure 1). This leads to the formation of phenoxy-radical, and the interaction between TBEC and TAIC is stopped [20].

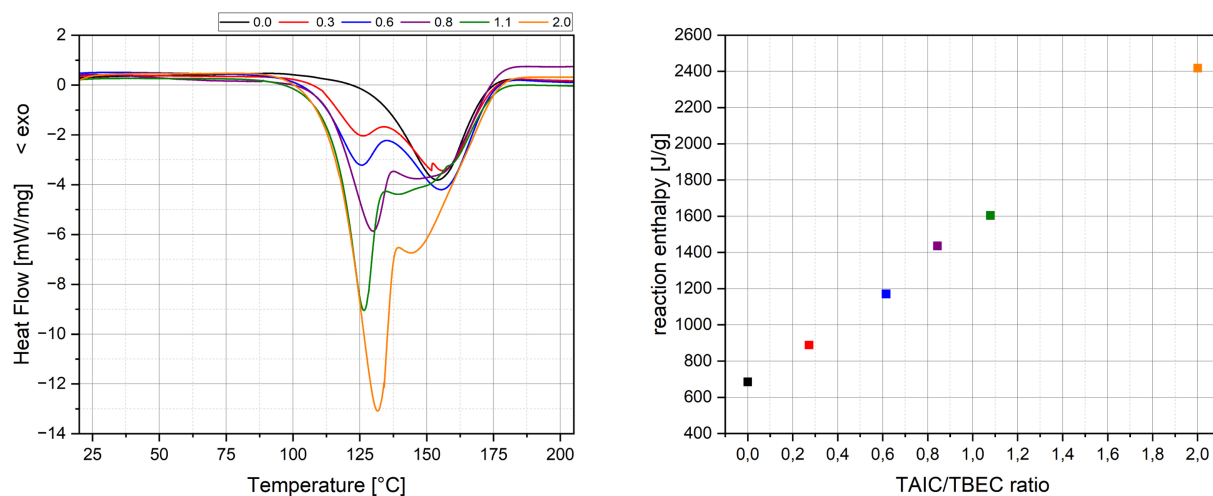


FIGURE 2 | Heat flow (left) and reaction enthalpies (right) during DSC experiments with TAIC-TBEC mixtures. The ratio in the heat flow legend is based on the quotient of TAIC/TBEC. The curves have been normalized to the mass of TBEC.

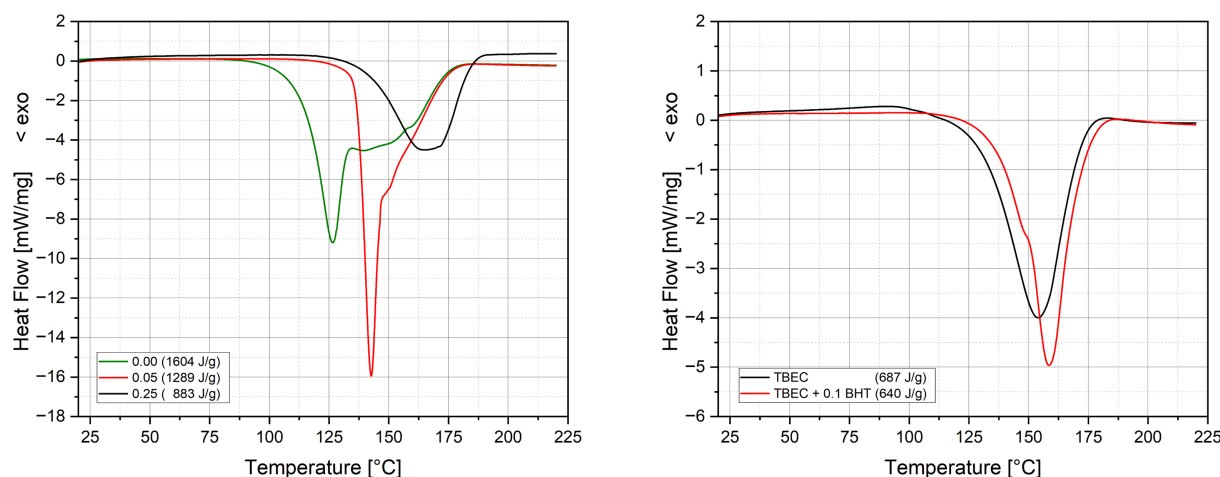


FIGURE 3 | Heat flow and reaction enthalpies during DSC experiments with TBEC-TAIC-BHT mixtures (left) and the influence of BHT on plain TBEC (right). TAIC/TBEC proportions are 1:1.

The comparison between TBEC without and with addition of 1/10 BHT based on the TBEC content showed that the influence on decomposition is only minor. The reaction heat decreases from 685 to 640 J/g, while the peak maximum temperature increases from 154.0°C to 158.5°C. It can therefore be assumed that the main point of attack of BHT must be the radicalized form of TAIC.

3.2 | Quantification of Crosslinking Additives in EVA

There are several works which list the mass fractions of crosslinking additives for EVA encapsulants [3, 5–8]. However, these are generally based on data from the Flat Plate Array Project, which dates back 40 years [6]. At present, the mass fractions of crosslinking additives used in the industry are largely unknown. In the past, a method was developed to quantify UV additives in EVA encapsulants [3]. This method was further expanded and transferred to crosslinking additives. The data and methodology are based on [4]. All used encapsulant compositions and the methodology to quantify crosslinking additives in EVA are explained in detail in [4] and the [supporting information](#) of this work.

It has to be mentioned that Luperox TBEC cannot be quantified directly. The peroxide is thermally unstable and decomposes during the 300°C desorption step [17, 18]. However, the fragment 2-Ethylhexan-1-ol is formed during the thermal decomposition of Luperox TBEC and is in a stoichiometric ratio to the base molecule. Consequently, the decomposition product can be correlated with the mass fraction of the crosslinking peroxide and used for quantification. A detailed chromatogram with the decomposition of Luperox TBEC and the peak intensity in dependence of the Luperox TBEC content is shown in the [supporting information](#) and in [4].

By using the calibration samples produced (see [supporting information](#)), it was possible to quantify the crosslinking peroxide Luperox TBEC and the crosslinking accelerator Perkalin

301 (TAIC) in commercial EVA films. The results are shown in Figure 4. In the various EVA films, Luperox TBEC between 0.6% and 1.25% mass contents were detected. It should be noted that the only difference between EVA 4 and EVA 5 was the presence of an UV absorber. Perkalin 301 was detected in the encapsulants with mass fractions of approximately 0.06% to 0.125%. This means that partially significantly lower amounts of crosslinking peroxide are used in EVA films today (see 1.5% to 3.0% in the flat-plate array project) [6–8]. Furthermore, significantly less crosslinking accelerator is used than crosslinking peroxide. This supports the consideration that crosslinking accelerator provides bonds between the polymer chains during peroxide crosslinking processes by hydrogen abstraction [17–19, 22, 23, 34, 35]. Since the crosslinking accelerator must also react with the radicals of the crosslinking peroxide, at least 2 Luperox TBEC molecules are required to link two polymer chains by means of one Perkalin 301 molecule. Since it cannot be assumed that the polymer chains and crosslinking accelerator molecules are always perfectly arranged within the polymer matrix (i.e., radical positions are close to each other to recombine) and the peroxide could also decompose with the formation of CO₂, probably significantly more crosslinking peroxide than crosslinking accelerator is required to initiate crosslinking.

3.3 | Crosslinking Behavior of EVA With Varying Additive Contents

The previously gained knowledge of the pure substances and the additive contents determined by PY-GCMS quantification are now transferred to self-produced films with variable TBEC and TAIC contents. The Evatane 28-25 polymer matrix used for this purpose does not contain BHT in order to avoid the influence of antioxidants on the crosslinking behavior shown in Section 3.1.

Figure 5 shows the DSC curves in the temperature interval of the crosslinking reaction of different TBEC-TAIC ratios in EVA and the corresponding reaction enthalpy. As it will be shown later, the 0.75% w/w TBEC series is a promising candidate for sufficient GCs. The measurements of the film samples show a

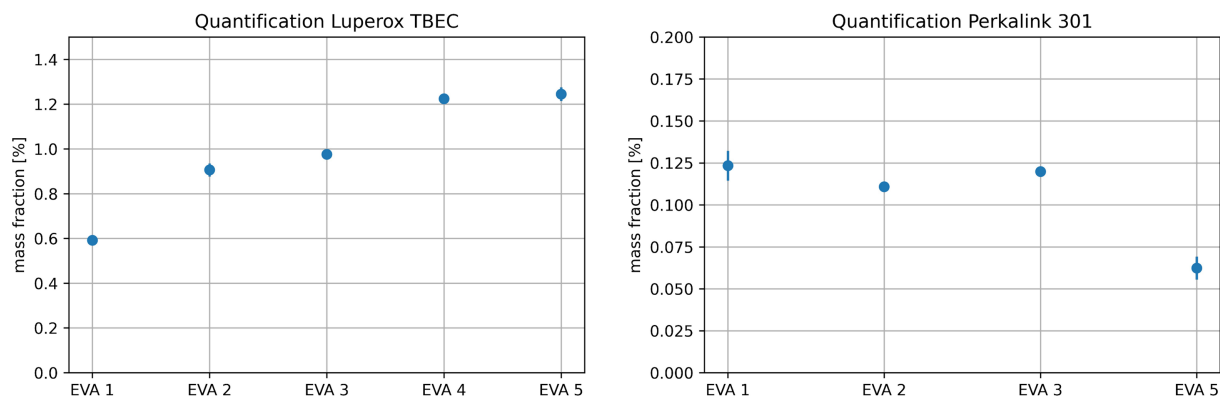


FIGURE 4 | Quantification of the crosslinking peroxide Luperox TBEC (left) and the crosslinking accelerator Perkalink 301 (TAIC - right) in different commercial EVA films. The original trade names have been replaced by general terms. The methodology is in accordance with [3, 4]. The error bars indicate the standard deviation of three measurements. The graphs are taken from [4].

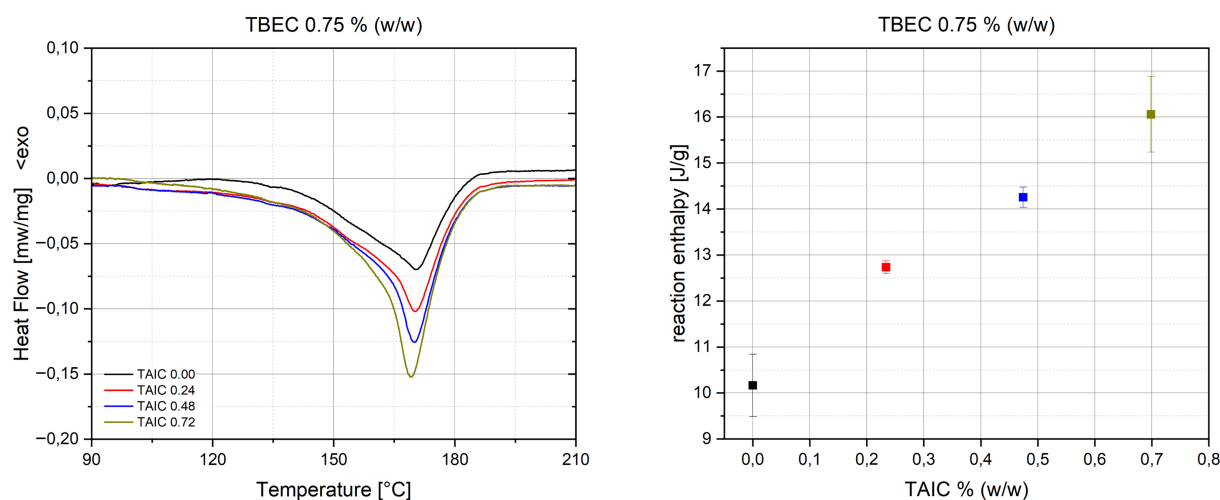


FIGURE 5 | Heat flow (left) and reaction enthalpies (right) during DSC experiments with different TAIC-TBEC ratios in EVA. The curves have been normalized to the mass of the EVA sample.

similar trend to the analyses of the pure substances in Figure 2. The reaction enthalpy for pure TBEC with a content of 0.75% w/w is approximately 10.2J/g. With the addition of TAIC, the reaction enthalpy increases in a linear ratio up to 16 J/g for a TAIC content of 0.7% w/w. With increasing the amount of TAIC, the peak maximum temperature of the exothermic crosslinking reaction decreases (see [supporting information](#) for a detailed graph). This could make it possible to reduce the process temperatures during lamination. All films were laminated with a lamination time of 20min. After lamination, the samples with the highest peroxide content show no exothermic peaks in the DSC measurements (see SI). It can therefore be assumed that all crosslinking peroxides have reacted during lamination and the measured reaction enthalpy of the raw samples represents the complete crosslinking process of the EVA films. Although there is a correlation between reaction enthalpy and GC achieved (see GC data for this film series in the SI), it is shown below that GCs can be generated in different ways (combinations of TBEC and TAIC). Even though there are works that correlate the GC via the reaction enthalpy [35], the direct measurement using solvent swelling is used in the following to determine the dependence on the additive concentrations used beyond doubt.

The left image of Figure 6 visualizes the achieved GC (mean of three measurements—see SI) for polymer film compositions varying the TBEC content from 0.00% w/w to 1.45% w/w and the TAIC content from 0.00% w/w to 0.70% w/w, while the right image is a linear interpolation of the measurement points indicating GC sections in dependence of the additive composition. All used additive concentrations and the corresponding GC are displayed in the [supporting information](#).

The graph shows that the GC can be increased in various ways. However, as shown in section Section 3.1 (and in previous experiments), a minimum amount of crosslinking peroxide is always necessary to initiate the crosslinking process. If the TBEC content is varied from 0.49% w/w to 1.45% w/w without the use of TAIC, GCs from 24.42% to 88.89% can be achieved. About 0.24% w/w TBEC did not lead to a measurable GC as the polymer chains have been completely dissolved. Even with Soxhlet extraction carried out on the basis of IEC 62788-1-6 but using toluene as a solvent [30], no mass changes could be observed. However, DSC measurements (see SI) show a small exothermic reaction peak indicating a weak crosslinking reaction. If a TBEC content of approximately 0.74% w/w is used, the required

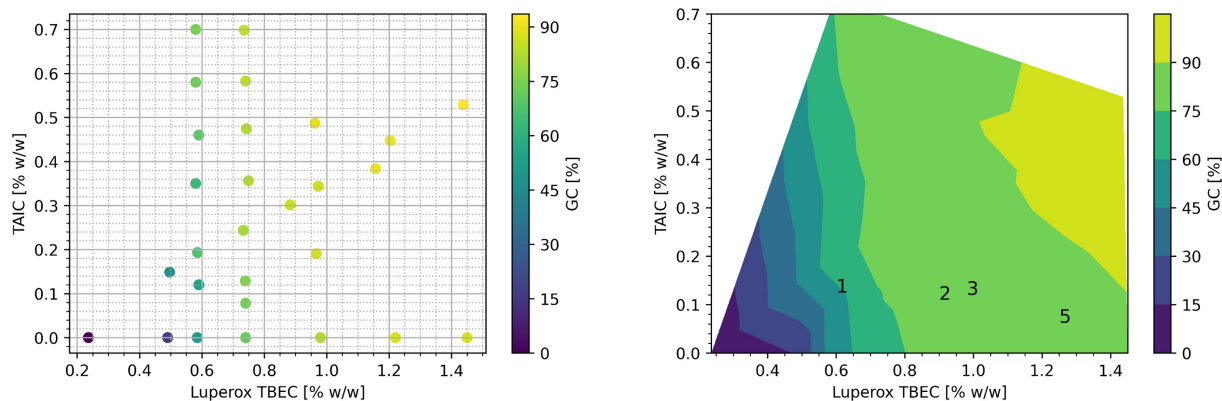


FIGURE 6 | Maximum achievable GC of different EVA films after 20min lamination in dependence of the TAIC and TBEC proportions (left) and interpolated regions of the resulting GC in dependence of the additive mixture (right) with the contents of the commercial EVA 1, EVA 2, EVA 3, and EVA 5. The interpolation was carried out using the *griddata* module from *scipy.interpolate* in *Python 3.9.7*.

minimum GC of $> 70\%$ is reached. However, this minimum value can also be achieved for TBEC contents of 0.58% w/w if TAIC is added in the same mass ratio. If TAIC is added to the TBEC mixed with 0.74% w/w, the GC can be further increased. If a TAIC content of approximately 0.36% w/w is used, the GC is about 82%. With a further increase in TAIC, however, the GC quickly reaches saturation. In the case of the crosslinking reaction during lamination, TAIC only provides additional bonds, so the molecule must also react with the peroxide and increasing the TAIC content alone is not effective. GCs around 90% can only be achieved with different combinations of TBEC and TAIC. For example, a mixture with 0.96% w/w TBEC and 0.47% w/w TAIC can achieve almost the same GC (approximately 90%) as a combination of 1.16% w/w TBEC and 0.38% w/w TAIC.

Based on the measured data, GC intervals can be interpolated, which can be achieved by different combinations of TBEC and TAIC for the polymer matrix and lamination conditions used. If TBEC percentages of over 0.80% w/w are used, GC values of over 75% can usually be achieved. In general, all TBEC values are in the range of the commercial films shown in Section 3.2. However, EVA 5 (and EVA 4) in particular use a comparatively high TBEC and low TAIC value. As shown in other studies, this entails the risk of subsequent reaction of the crosslinking peroxides if they were not completely consumed during lamination [5, 12, 26, 27]. With the exception of EVA 1 (GC = 85.8%), EVA 2 (GC = 82.2%), EVA 3 (GC = 83.8%), and EVA 5 (GC = 87.0%) show good agreement with the expected GC intervals from the interpolation. The deviation of EVA 1 could be due to the fact that additional (or other) crosslinking additives were used that could not be detected by PY-GCMS. On the other hand, the EVA matrix used could differ too much from Evatane 28-25, so that a different set of calibration samples is required for additive quantification.

By further investigating the results of Figure 6, it is possible to predict the expected GC in dependence of the amounts of crosslinking additives used. For this purpose, the $GC(L, T)$ was expressed as a function of the Luperox TBEC mass fraction L and the TAIC mass fraction T . On the left side of Figure 7, the GC is

shown as a function of L and T . The measurement points were approximated using a quadratic surface $GC_q(L, T)$ and a cubic surface $GC_c(L, T)$ (see SI). Consequently, the basic polynomial forms depending on two variables result in

$$GC_q(L, T) = a + bL + cT + dL^2 + eT^2 + fLT, \quad (2)$$

$$GC_c(L, T) = a + bL + cT + dL^2 + eT^2 + fLT + gL^3 + hT^3 + iL^2T + jLT^2, \quad (3)$$

with the coefficients $a, b, c, d, e, f, g, h, i, j$ listed in Table 2. Both surfaces describe the measuring points accurate and result in coefficients of determination (r^2 values) of 0.941 for the quadratic approximation and 0.954 for the cubic approximation. The mean absolute error (MAE) for predicting GC values is 3.466% for the quadratic function and 3.336% for the cubic function. Further images of the quadratic approximation and images of the cubic approximation can be found for different viewing angles in the [supporting information](#).

Both polynomials were used to predict the GC contents of three validation films with different mass fractions of Luperox TBEC and TAIC. The results are shown in the right graph of Figure 7. As it can be seen from the verification samples, the GC for the crosslinking system and the polymer matrix used can be predicted approximately with both fits. Since the quadratic surface also provides good accuracy for low GC contents, but significantly fewer measuring points are required to determine the coefficients (see Table 2), this approximation is suitable if one wants to optimize the crosslinking system. In this way, it can be estimated with comparatively little effort what minimum mass fractions of the crosslinking additives are required to achieve GC of at least 70% (under the same lamination conditions). As the quadratic plane has only one maximum, it becomes less accurate for high GC. Consequently, a combination of cubic and quadratic surfaces is useful to estimate a wider range of additive mixtures and their influence on the GC.

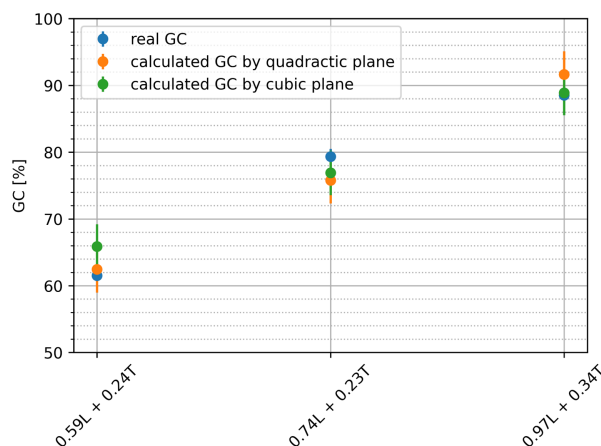
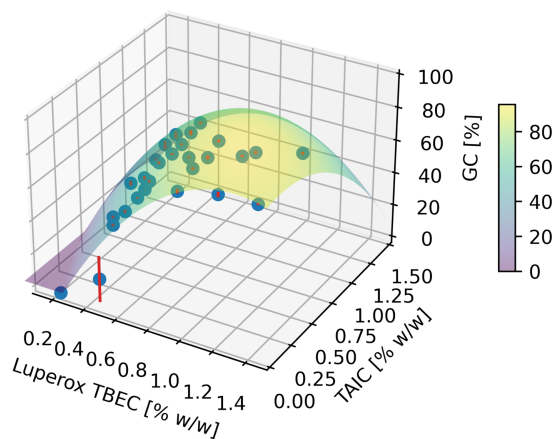


FIGURE 7 | Quadratic plane approximation of all GC measurement points from Figure 6 in dependence of the used additive compositions (left, see SI for further images) and calculated GC of polymer films using different additive compositions by quadratic and cubic approximations (right). The error bar expresses the standard deviation of the GCs. The fit was carried out using the *griddata* module from *scipy.interpolate* and the *curve_fit* module from *scipy.optimize* in Python 3.9.7.

TABLE 2 | Coefficients for Equations (2) and (3) to describe the plane and obtain the results in Figure 7.

Coefficient	Quadratic plane	Cubic plane
a	-48.19	-46.39
b	212.23	177.97
c	101.6	301.34
d	-81.02	-17.27
e	-42.77	-400.54
f	-58.63	-335.8
g		-29.03
h		166.92
i		73.77
j		266.62
r^2	0.941	0.954
MAE (%)	3.466	3.336

Note: r^2 is the coefficient of determination and MAE describes the mean absolute error.

3.4 | Impact of the Lamination Temperature

The temperature chosen for crosslinking has a decisive influence on the polymer properties [18]. To investigate the influence of temperature on the GC, laminations were carried out at three different temperatures. As a standard, 155°C was chosen based on a commercial encapsulant data sheet. This lamination temperature was varied by $\pm 10^\circ\text{C}$ to investigate the influence on the crosslinking behavior. The holding time was fixed at 20 min in each case to give the peroxide crosslinker sufficient time to react. From the results found in the previous sections, the two TBEC contents 0.6% w/w and 0.75% w/w were investigated in more detail as both could potentially reach the desired minimum of 70% GC by varying the TAIC

content. Figure 8 shows the achieved GC in dependence of the additive concentrations. As it can be seen in the graphs, the lamination temperature has a major influence on the expected GC for all TBEC-TAIC ratios.

The decomposition rate of the peroxide increases at higher temperatures. This also increases the reaction rate, which has a direct influence on crosslinking when the holding time is constant [36]. The comparison between 155°C (standard temperature) and 165°C shows that for the lower TBEC concentration (0.6% w/w), an increase in GC of 8% without the presence of the crosslinking accelerator TAIC can be achieved. The gradual increase in the share of TAIC leads to a further increase in GC. As already described, this can be explained by the active participation of TAIC in the crosslinking process while higher temperatures may increase the path length of the molecules and their reactions kinetics. This creates additional bonding sites between the polymer chains, which has a positive effect on the 3D network formed. At a TAIC content of approximately 0.6% w/w, a plateau formation occurs which is in accordance with the previous considerations that TAIC on its own does not influence the GC. The determined GC at this point is 82%.

The target for sufficient crosslinking of EVA-based encapsulation film is $> 70\%$ [12]. This could be achieved by increasing the lamination temperature. A comparison measurement with 0.75% w/w shows a similar behavior. An increase in GC with increasing temperature as well as the enhancement by TAIC addition is also evident. As the lamination time should be long enough for all peroxides to react, the higher GC represents a higher crosslinking reaction yield as less side reactions (i.e., the formation of CO_2) occur. The starting values without TAIC are already 21% (155°C) and 15% (165°C) higher than with the reduced TBEC content. This clearly shows the influence of the peroxide content on the degree of crosslinking. GC values $> 80\%$ can already be achieved with 0.24% w/w TAIC and thus confirm the additive contents in commercial films determined in Section 3.2. Thus, by tuning the lamination temperature and TAIC content, the

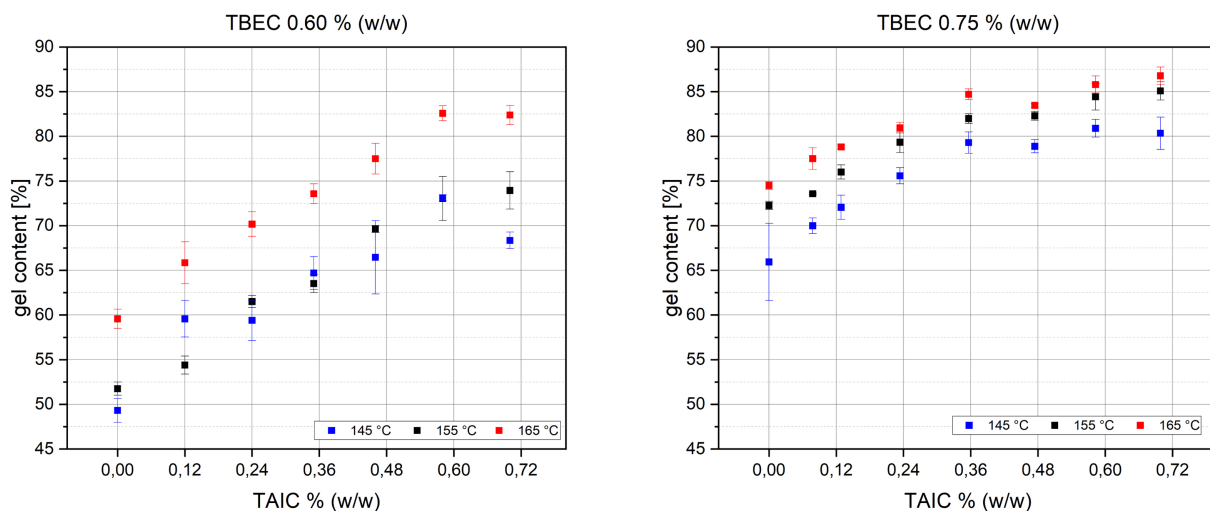


FIGURE 8 | Influence of the lamination temperature on the achieved GC with different TAIC contents using 0.60% w/w TBEC (left) and 0.75% w/w TBEC (right).

peroxide content can be greatly reduced minimizing the risks of undesired side reactions.

4 | Conclusion

The experiments carried out have revealed some fundamental relationships in the peroxide crosslinking of EVA encapsulants used for the PV industry. The interaction of crosslinking peroxide and crosslinking accelerator has a major influence on the reaction enthalpy, the GC, and the temperature at which lamination is most suitable. However, it could also be shown that stabilizing additives such as BHT can have a negative effect on the reaction enthalpy. It was observed that the antioxidant used probably does not react with the peroxide itself but with the crosslinking accelerator converted to a radical, which serves as a bridge between different polymer chains.

For the first time, crosslinking additives in commercial films were quantified using PY-GCMS. Based on this data, EVA films with different TBEC and TAIC could be produced iteratively. The GC measurements of these films showed that at least 0.8% w/w crosslinking peroxide should be used to achieve a GC of > 75% under the lamination conditions used. By using TAIC, less TBEC can be used and the peak maximum temperature (lamination temperature) decreases. A comparison with commercial films has shown that some of these use more peroxide, which can lead to undesirable side reactions. It is even possible to predict the expected GC depending on the proportion of crosslinking additives by fitting a large set of different GCs.

Furthermore, it was observed that the lamination temperature has a major influence on the expected GC under otherwise identical conditions (pressure, holding time, etc.). For example, when using only 0.60% w/w TBEC and 0.35% w/w TAIC, the GC could be increased from 63% to 73%, if the lamination temperature is increased from 155 °C to 165 °C.

Author Contributions

M.W. carried out the experiments (except PY-GCMS measurements), analyzed the data, discussed the results, writing-original draft, and reviewed the manuscript. P.W. and R.G. discussed the results and reviewed the manuscript. A.M. discussed the results and reviewed the manuscript, project supervision. R.H. carried out the PY-GCMS measurements, analyzed the data, discussed the results, writing-original draft, and reviewed the manuscript, project supervision.

Acknowledgments

This work was supported by TotalEnergies. Open Access funding enabled and organized by Projekt DEAL.

Conflicts of Interest

The author declares no conflicts of interest.

References

1. A. W. Czanderna and F. J. Pern, "Encapsulation of PV Modules Using Ethylene Vinyl Acetate copolymer as a pottant: A critical review," *Solar Energy Materials and Solar Cells* 43, no. 2 (1996): 101–181.
2. M. C. C. de Oliveira, A. S. A. D. Cardoso, M. M. Viana, and V. F. C. Lins, "The Causes and Effects of Degradation of Encapsulant Ethylene Vinyl Acetate Copolymer (EVA) in Crystalline Silicon Photovoltaic Modules: A Review," *Renewable and Sustainable Energy Reviews* 81 (2018): 2299–2317.
3. R. Heidrich, A. Mordvinkin, and R. Gottschalg, "Quantification of UV Protecting Additives in Ethylene-Vinyl Acetate Copolymer Encapsulants for Photovoltaic Modules With Pyrolysis-Gas Chromatography-Mass Spectrometry," *Polymer Testing* 118 (2023): 107913.
4. R. Heidrich, "Encapsulation Polymer Degradation and Its Impact on the Deterioration of Solar Modules" (Unpublished doctoral thesis, 2024).
5. R. Heidrich, M. Lüdemann, A. Mordvinkin, and R. Gottschalg, "Diffusion of UV Additives in Ethylene-Vinyl Acetate Copolymer Encapsulants and the Impact on Polymer Reliability," *IEEE Journal of Photovoltaics* (2023).

6. E. Cuddihy, C. Coulbert, A. Gupta, and R. Liang, "Flat-Plate Solar Array Project: Final Report: Volume 7, Module Encapsulation," Jet Propulsion Lab., Pasadena, CA (USA), (1986).
7. C. Peike, L. Purschke, K.-A. Weiss, M. Köhl, and M. Kempe, "Towards the Origin of Photochemical EVA Discoloration," in *2013 IEEE 39th Photovoltaic Specialists Conference (PVSC)*, (IEEE, 2013): 1579–1584.
8. A. Beinert, C. Peike, I. Dürr, M. D. Kempe, G. Reiter, and K.-A. Weiß, "The Influence of the Additive Composition on Degradation Induced Changes in Poly (Ethylene-Co-Vinyl Acetate) During Photochemical Aging," in *29th European PV Solar Energy Conference and Exhibition, Amsterdam*, (2014).
9. C. Barretta, G. Oreski, S. Feldbacher, K. Resch-Fauster, and R. Pantani, "Comparison of Degradation Behavior of Newly Developed Encapsulation Materials for Photovoltaic Applications Under Different Artificial Ageing Tests," *Polymers* 13, no. 2 (2021): 271.
10. R. Heidrich, N. Babić, O. Lacroix-Andrivet, et al., "From Performance Measurements to Molecular Level Characterization: Exploring the Differences Between Ultraviolet and Damp Heat Weathering of Photovoltaics Modules," *Solar RRL* 8, no. 10 (2024): 2400144.
11. R. Heidrich, C. Barretta, A. Mordvinkin, G. Pinter, G. Oreski, and R. Gottschalg, "UV Lamp Spectral Effects on the Aging Behavior of Encapsulants for Photovoltaic Modules," *Solar Energy Materials and Solar Cells* 266 (2024): 112674.
12. G. Oreski, A. Rauschenbach, C. Hirschl, M. Kraft, G. C. Eder, and G. Pinter, "Crosslinking and Post-Crosslinking of Ethylene Vinyl Acetate in Photovoltaic Modules," *Journal of Applied Polymer Science* 134, no. 23 (2017): 44912.
13. C. Hirschl, L. Neumaier, W. Mühleisen, et al., "In-Line Determination of the Degree of Crosslinking of Ethylene Vinyl Acetate in PV Modules by Raman Spectroscopy," *Solar Energy Materials and Solar Cells* 152 (2016): 10–20.
14. M. Halwachs, L. Neumaier, N. Vollert, et al., "Statistical Evaluation of PV System Performance and Failure Data Among Different Climate Zones," *Renewable Energy* 139 (2019): 1040–1060.
15. S. Jonai, K. Hara, Y. Tsutsui, H. Nakahama, and A. Masuda, "Relationship Between Cross-Linking Conditions of Ethylene Vinyl Acetate and Potential Induced Degradation for Crystalline Silicon Photovoltaic Modules," *Japanese Journal of Applied Physics* 54, no. 8S1 (2015): 8KG01.
16. A. Omazic, G. Oreski, M. Halwachs, et al., "Relation Between Degradation of Polymeric Components in Crystalline Silicon PV Module and Climatic Conditions: A Literature Review," *Solar Energy Materials and Solar Cells* 192 (2019): 123–133.
17. S. Mishra, B. Baweja, and R. Chandra, "Studies on Dynamic and static Crosslinking of Ethylene Vinyl Acetate and Ethylene Propylene Diene Tercopolymer Blends," *Journal of Applied Polymer Science* 74, no. 11 (1999): 2756–2763.
18. H. A. Khonakdar, J. Morshedian, U. Wagenknecht, and S. H. Jafari, "An Investigation of Chemical Crosslinking Effect on Properties of High-Density Polyethylene," *Polymer* 44, no. 15 (2003): 4301–4309.
19. S. Muroga, Y. Takahashi, Y. Hikima, S. Ata, M. Ohshima, T. Okazaki, and K. Hata, "New Evaluation Method for the Curing Degree of Rubber and Its Nanocomposites Using ATR-FTIR Spectroscopy," *Polymer Testing* 93 (2021): 106993.
20. H. Zweifel, *Stabilization of Polymeric Materials* (Springer Science and Business Media, 2012).
21. W. Lai, C. Li, H. Chen, and S. Shaik, "Hydrogen-Abstraction Reactivity Patterns From A to Y: The Valence Bond Way," *Angewandte Chemie International Edition* 51, no. 23 (2012): 5556–5578.
22. R. Anbarasan, O. Babot, and B. Maillard, "Crosslinking of High-Density Polyethylene in the Presence of Organic Peroxides," *Journal of Applied Polymer Science* 93, no. 1 (2004): 75–81.
23. E. Passaglia, S. Coiai, G. Giordani, E. Taburoni, L. Fambri, V. Pagani, and M. Penco, "Modulated Crosslinking of Polyolefins Through Radical Processes in the Melt," *Macromolecular Materials and Engineering* 289, no. 9 (2004): 809–817.
24. W. Stark and M. Jaunich, "Investigation of Ethylene/Vinyl Acetate Copolymer (EVA) by Thermal Analysis DSC and DMA," *Polymer Testing* 30, no. 2 (2011): 236–242.
25. B. S. Chernev, C. Hirschl, and G. C. Eder, "Non-Destructive Determination of Ethylene Vinyl Acetate Cross-Linking in Photovoltaic (pv) Modules by Raman Spectroscopy," *Applied Spectroscopy* 67, no. 11 (2013): 1296–1301.
26. P. Klemchuk, M. Ezrin, G. Lavigne, W. Holley, J. Galica, and S. Agro, "Investigation of the Degradation and Stabilization of EVA-Based Encapsulant in Field-Aged Solar Energy Modules," *Polymer Degradation and Stability* 55, no. 3 (1997): 347–365.
27. N. Pinochet, R. Couderc, and S. Therias, "Solar Cell UV-Induced Degradation or Module Discolouration: Between the Devil and the Deep Yellow Sea," *Progress in Photovoltaics: Research and Applications* 31, no. 11 (2023): 1091–1100.
28. D. Wu, P. Wessel, J. Zhu, D. Montiel-Chicharro, T. R. Betts, A. Mordvinkin, and R. Gottschalg, "Influence of Lamination Conditions of EVA Encapsulation on Photovoltaic Module Durability," *Materials* 16, no. 21 (2023): 6945.
29. A. Badiie, I. A. Ashcroft, and R. D. Wildman, "The Thermo-Mechanical Degradation of Ethylene Vinyl Acetate Used as a Solar Panel Adhesive and Encapsulant," *International Journal of Adhesion and Adhesives* 68 (2016): 212–218.
30. IEC 62788-1-6:2017, "Measurement Procedures for Materials Used in Photovoltaic Modules - Part 1-6: Encapsulants - Test Methods for Determining the Degree of Cure in Ethylene-Vinyl Acetate," International Electrotechnical Commission, (2017).
31. M. Jaunich, M. Böhning, U. Braun, G. Teteris, and W. Stark, "Investigation of the Curing State of Ethylene/Vinyl Acetate Copolymer (EVA) for Photovoltaic Applications by Gel Content Determination, Rheology, DSC and FTIR," *Polymer Testing* 52 (2016): 133–140.
32. "Plastics - Differential Scanning Calorimetry (DSC) - Part 5: Determination of Characteristic Reaction-Curve Temperatures and Times, Enthalpy of Reaction and Degree of Conversion (ISO 11357-5:2013); German Version EN ISO 11357-5:2014," Deutsches Institut für Normung, (2017).
33. I. B. Talouba, L. Balland, N. Mouhab, and N. Bensahla, "Kinetic and Safety Parameters of Decomposition of Neat Tert-Butyl (2-Ethylhexyl) Monoperoxy Carbonate and in Organic Solvents," *Thermochimica Acta* 659 (2018): 105–112.
34. K. M. McLoughlin, A. J. Oskoue, M. K. Sing, A. Bandegi, S. Mitchell, J. Kennedy, T. G. Gray, and I. Manas-Zloczower, "Thermomechanical Properties Of Cross-Linked EVA: A Holistic Approach," *ACS Applied Polymer Materials* 5, no. 2 (2023): 1430–1439.
35. C. Hirschl, M. Biebl-Rydlo, M. DeBiasio, et al., "Determining the Degree of Crosslinking of Ethylene Vinyl Acetate Photovoltaic Module Encapsulants: A Comparative Study," *Solar Energy Materials and Solar Cells* 116 (2013): 203–218.
36. T.-K. Kang and C.-S. Ha, "Effect of Processing Variables on the Crosslinking of HDPE by Peroxide," *Polymer Testing* 19, no. 7 (2000): 773–783.

Supporting Information

Additional supporting information can be found online in the Supporting Information section.